

HOLE: Homological Observation of Latent Embeddings for Neural Network Interpretability

Sudhanva Manjunath Athreya*
University of Utah

Paul Rosen†
University of Utah

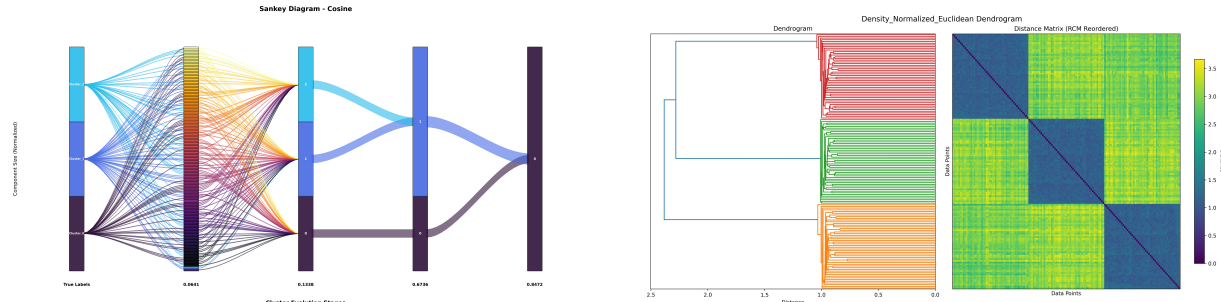


Figure 1: HOLE provides global interpretability via multiple visualization techniques: (left) Sankey flows (layer-wise representation changes) and (right) heatmap–dendograms (hierarchical structure).

ABSTRACT

Deep learning models have achieved remarkable success across various domains, yet their learned representations and decision-making processes remain largely opaque and hard to interpret. This work introduces HOLE (Homological Observation of Latent Embeddings), a method for analyzing and interpreting deep neural networks through persistent homology. HOLE extracts topological features from neural activations and presents them using a suite of visualization techniques, including Sankey diagrams, heatmaps, dendograms, and blob graphs. These tools facilitate the examination of representation structure and quality across layers. We evaluate HOLE on standard datasets using a range of discriminative models, focusing on representation quality, interpretability across layers, and robustness to input perturbations and model compression. The results indicate that topological analysis reveals patterns associated with class separation, feature disentanglement, and model robustness, providing a complementary perspective for understanding and improving deep learning systems.

Index Terms: Deep learning, explainable AI, persistent homology, topological data analysis, visualization.

1 INTRODUCTION

Deep learning models have gained popularity in recent years [25, 41], and have demonstrated remarkable predictive performance on a wide range of complex tasks, including computer vision [40] and natural language processing [15]. They are often considered to be black boxes, which presents significant challenges, including difficulty in debugging model failures, a lack of trust from end users, potential for perpetuating bias, and regulatory compliance issues [54, 63]. The fundamental problem underlying these issues is the lack of interpretability and explainability—we cannot understand what features the model has learned, how it processes information, or why it makes specific decisions, making it impossible

to debug, trust, or verify these systems effectively. This lack of interpretability has profound implications, as there is a rise in the deployment of AI models in critical sectors such as healthcare [60, 70] and finance [35, 46], where transparency, fairness, accountability, and ethical considerations are important [5, 51].

Multiple factors contribute to the difficulty in understanding these models. First, their complex architectures often involve millions of parameters, which leads to high-dimensional internal states. Second, the usage of non-linear activation functions results in complex decision spaces that are not intuitive. Third, over-parameterization of many architectures introduces challenges, as multiple configurations can yield similar performance while differing internally. Finally, the nature of the learned representations, i.e., concepts, is often distributed across numerous layers rather than being localized, and those concepts generally do not correspond to human-interpretable concepts, which limits transparency.

To address the interpretability challenges of deep learning models, we consider the application of persistent homology to the internal states of the model. Persistent homology captures the intrinsic topological structure of high-dimensional data by identifying and quantifying features such as connected components and loops across multiple scales, without performing a lossy dimension reduction operation. Moreover, a significant advantage of persistent homology is its model-agnostic nature and robustness to noise, rendering it broadly applicable across diverse neural network architectures. By applying this technique to the internal activations or learned representations of neural networks, it becomes possible to characterize how information is organized and transformed across layers. This topological perspective can reveal stable and significant patterns that are invariant to specific parameterizations, offering insights into the global structure of representations and potentially identifying meaningful, interpretable features. As a result, persistent homology provides a principled way to analyze the internal complexity of deep models beyond conventional feature-space visualization or attribution methods.

In this work, we present HOLE (Homological Observation of Latent Embeddings), a python library for interpreting and analyzing neural networks using persistent homology. To reveal the nuanced structure of high-dimensional activation spaces, HOLE performs filtrations using multiple distance metrics, including Euclidean, Co-

*e-mail: sud.athreya@utah.edu

†e-mail: paul.rosen@utah.edu

sine, Mahalanobis, and geodesic distances, each designed to highlight different geometric and semantic properties of the learned representations. The resulting topological data is made interpretable through a suite of visualization techniques, including dendograms, heatmaps, blob graphs, and Sankey-based diagrams that trace the evolution of clusters across layers. Furthermore, we demonstrate HOLE’s utility by demonstrating its ability to reveal learned representations, and in assessing model integrity by analyzing its robustness to common corruptions like input noise and the structural impacts of compression techniques such as pruning and quantization. By examining the stability of topological features under these conditions, HOLE provides insights into model behavior beyond traditional accuracy metrics, offering a more holistic understanding of a model’s representational quality and potential failure modes.

2 RELATED WORKS

Computational topology techniques have gained popularity in data analysis in the last few years, including for understanding neural representations [58].

2.1 Topological Data Analysis and Visualization

Recent advances in topological data analysis [66] have demonstrated that studying the shape and topological structure of data in high-dimensional spaces provides powerful insights into underlying patterns. Specifically, *persistent homology* has emerged as a powerful mathematical framework for quantifying the persistence of topological features across multiple scales [18, 77]. The output of persistence homology, called persistence diagrams, is stable under perturbations of the input [13], which opened the door to applications in noisy settings.

The persistence information is visualized using a scatterplot-like visualization, somewhat confusingly called a persistence diagram, or a barchart-like visualization, called a persistence barcode [24], which provides compact representations of the birth and death times of topological features across different scales (Fig. 2). Vector-space representations such as persistence landscapes [9] have been proposed to transform persistence diagrams into a function-based representation in a vector space, making them usable in machine learning and statistical analysis. Other approaches include persistence images, which create a fixed-size vector representation from diagrams, and specialized kernels [11]. These methods, along with scalable software libraries (e.g., GUDHI [50]), provide practical access to topological methods.

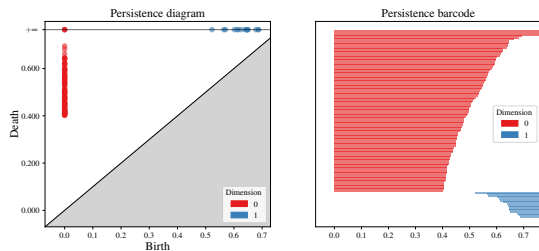


Figure 2: Example (left) persistence diagram and (right) barcode.

A particularly influential method is *Mapper* [66], which constructs simplified representations of high-dimensional data by creating nerve complexes of overlapping neighborhoods. Unlike persistent homology, which focuses on quantifying the lifetime of topological features across scales, Mapper addresses the complementary problem of *shape summarization*—creating interpretable, graph-based visualizations that preserve the topological structure of the data while allowing interactive exploration.

2.2 Machine Learning Interpretability

The growing complexity of machine learning models has sparked significant interest in interpretability and explainability methods, which can be broadly categorized into local and global approaches. Activation maximization [19] and its variants generate synthetic inputs that reveal preferred stimuli for individual neurons or layers. Local explanation methods focus on understanding individual predictions. LIME (Local Interpretable Model-agnostic Explanations) [61] provides local explanations by learning interpretable models around individual predictions, offering insights into model behavior for specific instances. SHAP (SHapley Additive exPlanations) [49] builds on cooperative game theory to assign importance values to features, providing a unified framework that encompasses several existing explanation methods. Network dissection [6] systematically identifies neurons that correspond to interpretable concepts by measuring alignment with segmentation masks. TCAV (Testing with Concept Activation Vectors) [36] enables testing of user-defined concepts within neural networks, allowing researchers to probe whether models have learned human-interpretable concepts. Global explanation methods aim to understand model behavior more broadly. Feature visualization techniques [57] synthesize inputs that maximally activate specific neurons, revealing what patterns different parts of the network have learned to detect.

Saliency Maps and Gradient-Based Methods Saliency maps represent one of the most widely used approaches for explaining neural network predictions in computer vision. These methods highlight the regions of an input image that most strongly influence the model’s decision. The fundamental approach computes gradients of the output with respect to the input to identify important pixels or regions. Grad-CAM [64] generates visual explanations for CNN decisions by using gradients to produce coarse localization maps highlighting important regions in images. Unlike pixel-level gradient methods, Grad-CAM operates at the feature map level, providing more interpretable visualizations that show which parts of an image the network focuses on for specific predictions. Other gradient-based saliency methods include vanilla gradients, integrated gradients, and guided backpropagation, each offering different perspectives on input attribution. Integrated gradients [68] addressed gradient saturation issues by accumulating gradients along a path from a baseline to the input. SmoothGrad [67] improved saliency map quality by averaging gradients over multiple noisy versions of the input. Layer-wise Relevance Propagation (LRP) [2] proposed a principled approach to decompose predictions into relevance scores for individual features. Occlusion sensitivity analysis [76] provided a complementary approach by systematically blocking image regions to measure their impact on predictions. While saliency maps excel at providing intuitive visual explanations, they primarily focus on input-level attribution and may not capture the complex relationships.

Visualization Task Taxonomies Understanding user analytic activities has been a central concern in information visualization research. Amar et al. [1] identified ten low-level analytic primitives (retrieve value, filter, compute derived value, find extremum, sort, determine range, characterize distribution, find anomalies, cluster, and correlate) through empirical analysis of nearly 200 analyst questions across multiple domains. Their taxonomy emphasizes analytic primacy over representational primacy, arguing that visualization systems should be designed to support users’ analytic goals rather than merely presenting data. These primitives serve as foundational building blocks that can be composed into higher-level, domain-specific tasks. Our work builds upon this foundation by composing Amar et al.’s primitives into tasks specifically designed for persistent homology analysis of neural network activations, where tracking multi-scale topological evolution and assessing representation quality require coordinated application of multi-

ple primitive operations.

Interactive Visualization Systems The visualization community has also developed interactive tools for neural network analysis that complement traditional interpretability methods. Summit [32] presents an interactive system for scalable summarization and interpretation of deep neural networks, introducing activation aggregation to discover important neurons and neuron-influence aggregation to identify relationships between neurons. These techniques combine to create attribution graphs that reveal crucial neuron associations across network layers. ActiVis [34] provides visual exploration of industry-scale deep neural network models through coordinated views including computation graph overviews and neuron activation patterns. CNNVis [44] offers interactive visualization of convolutional neural networks, enabling users to explore learned features across different layers through multiple linked views. CNN Explainer [71] provides an educational tool with interactive visualizations that help novices understand the mathematical operations underlying CNNs.

These approaches have become foundational to explainable AI, enabling practitioners to understand and trust complex models. However, these methods primarily focus on feature-level explanations and may miss important structural patterns in learned representations. Our topological approach offers a complementary perspective by revealing the geometric and topological structure underlying model behavior and data representations, providing insights into how models organize and separate different classes of data.

2.2.1 Topology and Interpretability

During the last few years, there has been a convergence of topological data analysis and deep learning. Hofer et al. [31] showed how persistence can serve as a differentiable layer that preserves topological information in neural networks. Carrière et al. [12] built on this work with PersLay, developing a permutation-invariant architecture that can process persistence diagrams while maintaining their stability properties. Moor et al. [55] proposed topology-aware autoencoders that explicitly preserve the topological structure of data in the latent space, which provides explanation as to why the network represents the data in a certain way. These works indicate that several topological approaches can be used to improve the performance of neural networks. Rieck et al. [62] introduced Neural Persistence, which quantifies network complexity by analyzing the lifetime of connections in weight matrices. Improving on the previous work, Watanabe et al. [72] proposed layer-wise topological metrics to understand the complexity of networks at different depths. Purvine et al. [59] conducted detailed empirical studies of convolutional layer activations using topological methods, while Birdal et al. [7] established important connections between persistence and the intrinsic dimension of neural representations. Wheeler et al. [73] developed Activation Landscapes that provide a novel way to visualize and understand training trajectories.

Recent work has also revealed strong connections between topological features and model generalization. Gutierrez et al. [27] demonstrated that persistence statistics can estimate test performance without requiring a validation set, which is a strong indicator that topological features can be used to improve the performance of neural networks. Ballester et al. [3] then showed how these statistics can predict the generalization gap. Collectively, these works strengthen the evidence that topological priors can improve both performance and interpretability—an observation we leverage in the present paper. Rather than instance-level attributions, we pursue a global, layer-by-layer reading of a model’s internal organization—post hoc, comparative, and performed without altering the network. Topology contributes stable, scale-aware cues that make visible where semantic structure emerges, persists, or shifts across layers; we weave these cues into complementary multi-view summaries to support structure-aware explanation.

3 HOMOLOGICAL OBSERVATION OF LATENT EMBEDDINGS

Our approach involves observing the behavior of neural networks through the lens of persistent homology. Persistent homology is an interesting tool for this application because it can *summarize multi-scale structures in complex data, independent of the dimensionality, while being robust to certain types of noise*. We then construct several visualizations on top of persistent homology that are selected to reveal important structures in the neural network.

3.1 Deep Neural Network Structure and Data

Deep Neural Networks (DNNs) are computational graphs composed of layers and connections. A network consists of interconnected nodes called neurons, organized in a series of layers. Each layer outputs a weighted sum of its inputs, which is then followed by a nonlinear function known as an activation function. These activation functions (e.g., Sigmoid, Tanh, and ReLU) introduce nonlinearity to the networks. Without an activation function, the linear operations in the neural network can be collapsed into a single linear transformation. Thus, the mappings from the input to the output space become linear. To overcome this limitation, activation functions are placed after each linear transformation in the model. The outputs of these activation functions are considered “features” that a particular layer has learned. Interpretability methods often try to understand how a network creates decision boundaries in activation spaces. Therefore, the learned representations of the data can be found in these activations.

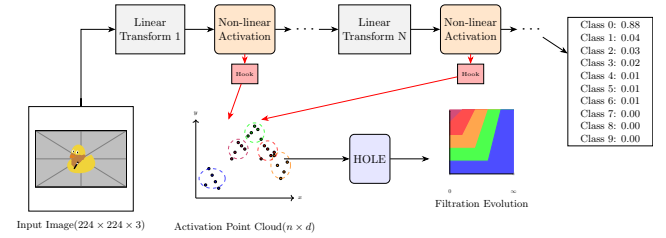


Figure 3: HOLE overview shows how during inference, neural network activations are extracted via forward hooks. These activations are passed as point clouds to the persistent homology function, and then the filtration process is visualized.

To understand the DNN’s internal data representations, we extract intermediate activations from the model as it processes input samples. We utilize multiple variations of the same input data, by introducing controlled variations, such as image augmentations, noise injection, or class-balanced sampling, we ensure that the extracted activations capture a wide range of the network’s representational capacity and robustness.

The forward hooks are placed into pre-selected non-linear layers of the network during inference, allowing us to record the outputs (i.e., activations) of these layers (Fig. 3). During inference, as each batch of input images is passed through the network, the forward hooks capture the activations at the specified layers. These activations are high-dimensional embeddings, which we reshape as needed to form vectors in \mathbb{R}^d , where d corresponds to the number of output units in the layer. The activations act as a point cloud for the downstream persistent homology analysis.

3.2 Persistent Homology

We employ persistent homology as our primary tool to analyze how the topological features of neural network activation point clouds evolve across the filtration.

Homology Let $X = \{x_1, x_2, \dots, x_n\} \subset \mathbb{R}^d$ be a finite point cloud (in our case neural network activations). A 0-simplex represents a vertex, a 1-simplex an edge, a 2-simplex a triangle, and

so forth. A *simplicial complex* K is a collection of simplices where every face of a simplex in K is also in K [10]. Formally, a k -simplex σ is the convex hull of $k+1$ affinely independent points:

$$\sigma = \{t_0v_0 + t_1v_1 + \dots + t_kv_k \mid t_i \geq 0, \sum_{i=0}^k t_i = 1\}$$

where v_0, v_1, \dots, v_k are the vertices. The k -th homology group $H_k(K)$ captures k -dimensional topological features: H_0 counts connected components, H_1 counts loops (holes), H_2 counts voids, etc. Formally, homology is defined through the chain complex:

$$\dots \xrightarrow{\partial_{k+1}} C_k(K) \xrightarrow{\partial_k} C_{k-1}(K) \xrightarrow{\partial_{k-1}} \dots \xrightarrow{\partial_1} C_0(K) \xrightarrow{\partial_0} 0$$

where $C_k(K)$ is the vector space of k -chains and ∂_k is the boundary operator. The k -th homology group is:

$$H_k(K) = \frac{\ker(\partial_k)}{\text{im}(\partial_{k+1})} = \frac{Z_k(K)}{B_k(K)}$$

where $Z_k(K)$ are k -cycles (closed chains) and $B_k(K)$ are k -boundaries. To construct simplicial complexes from point clouds, we utilize the *Vietoris-Rips (VR) complex* [18]. Given a distance function $d : X \times X \rightarrow \mathbb{R}$ and radius $\varepsilon \geq 0$, the VR complex is defined as:

$$\text{VR}_\varepsilon(X) = \{\sigma \subseteq X \mid \forall x_i, x_j \in \sigma, d(x_i, x_j) \leq \varepsilon\}$$

At a given radius ε , a k -simplex is formed among a set of points if pairwise distances are $\leq \varepsilon$.

Persistent Homology Persistent homology is a mathematical framework that allows tracking the evolution of topological features across different scales (i.e., values of ε) [10]. The key concept of persistent homology is a filtration, which is a growing sequence of metric balls, used to detect the size and scale of topological features of a dataset [17]. Mathematically, filtration can be defined as a nested sequence of simplicial complexes, $\emptyset = K_0 \subseteq K_1 \subseteq K_2 \subseteq \dots \subseteq K_m$, parameterized by increasing scale parameter $0 = \varepsilon_0 < \varepsilon_1 < \varepsilon_2 < \dots < \varepsilon_m$. As the filtration parameter ε increases, topological features appear, known as birth, and disappear, known as death. Persistent homology tracks these changes by computing homology groups across the filtration and recording birth-death pairs. Further, a measure, known as persistence, is the difference between the birth and the death values of a feature. Features with high persistence are considered significant topological structures, while short-lived features are typically attributed to noise.

To calculate persistent homology, we first calculate a pairwise distance matrix for the activation point cloud. We utilize multiple distance metrics in order to draw different interpretations of the network. We then we perform the filtration process on this distance matrix. In our case, we only need to track the clusters, so we compute the filtration up to dimension 1 (connected components).

3.3 Distance Metrics to Highlight Features

The distance metric is a crucial component of the filtration process. Each distance metric reveals a different geometric and semantic aspect of the learned representations. Fig. 4 shows the effects of the different distance metrics on synthetically generated data.

Euclidean Distance, or ℓ_2 -norm, is $d_{\ell_2}(x_i, x_j) = \|x_i - x_j\|_2$. This metric preserves absolute magnitudes and is sensitive to overall activation scale, making it suitable for analyzing how strongly neurons activate for different inputs.

Cosine Distance is $d_c(x_i, x_j) = 1 - \frac{x_i \cdot x_j}{\|x_i\| \|x_j\|}$, focusing on directional similarity while being invariant to magnitude. It is particularly effective for identifying semantic similarities when networks encode class information through consistent activation orientations.

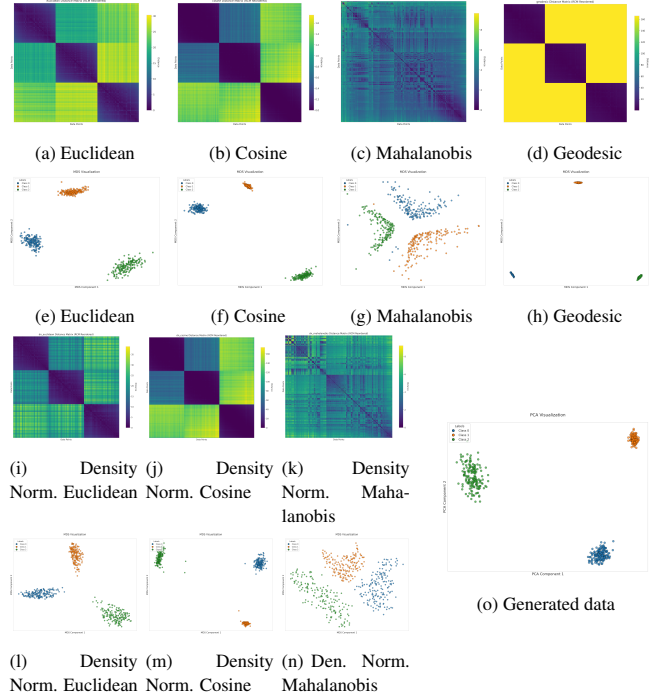


Figure 4: (o) The input dataset was used to generate (a-d,i-k) distance heatmaps and (e-h,l-n) MDS visualizations showing pairwise distances between the data points using various metrics.

Mahalanobis Distance, $d_m(x_i, x_j) = \sqrt{(x_i - x_j)^T \Sigma^{-1} (x_i - x_j)}$, incorporates covariance structure, accounting for feature correlations and anisotropic scaling. It can reveal cluster structures emerging from learned feature correlations and highlights how networks organize related concepts.

Geodesic Distance approximates intrinsic manifold distance by constructing a k -nearest neighbor graph $G = (V, E)$ and computing $d_g(x_i, x_j) = \min_{\gamma} \sum_{e \in \gamma} w(e)$, where γ is a path from x_i to x_j and $w(e)$ is the Euclidean weight of edge e . This captures non-linear relationships in curved or folded activation spaces.

Density-Normalization We can also apply relative neighborhood normalization to the data before Euclidean, Cosine, and Mahalanobis distances are calculated. For each point x_i , we define local scale μ_i as the average distance to its k nearest neighbors, yielding normalized distance $d_{ij} = \frac{d_{\text{base}}(x_i, x_j)}{\sqrt{\mu_i \mu_j}}$. This emphasizes local clustering patterns and provides robustness to outliers and global scale differences.

3.3.1 Metric Selection Guidelines

We performed an extensive evaluation of the utility of the various distance metrics. For the metric study, we generated synthetic datasets by crossing density (dense/sparse), separability (separable/non-separable), and outliers (on/off) for each structure family at fixed sample sizes and dimensionalities. For every variant we compute seven distance matrices: Euclidean, Cosine, Mahalanobis; density-normalized versions of each using k -nearest-neighbor local scales; and Geodesic via k -NN graph shortest paths. See appendix for additional details about the metric study.

Our systematic evaluation, summarized in Tab. 1, reveals that each distance metric excels in specific scenarios, with the choice depending on the underlying data characteristics and analysis objectives. Euclidean distance provides the most intuitive geometric

interpretation but fails when data contains outliers or lacks clear separation. Cosine distance offers robustness against outliers and focuses on directional relationships, making it ideal for semantic similarity analysis. Mahalanobis distance automatically accounts for feature correlations and variance structure, outperforming Euclidean distance for correlated data but at increased computational cost. Geodesic distance captures intrinsic manifold structure for non-linear data relationships, while density-normalized variants provide robustness against outliers by incorporating local scale information. The optimal metric selection should consider both the computational constraints and the specific topological features of interest in the activation space analysis.

Table 1: Summary of distance metric selection guidelines based on data characteristics and analysis goals.

Metric	Best For	Limitations
<i>Euclidean</i>	Isotropic, well-separated clusters; uniform density; small noise	Sensitive to outliers/scale; poor on curved manifolds
<i>Cosine</i>	Directional similarity in high-dim activations; varying magnitudes	Ignores magnitude; unstable near zero-norm vectors
<i>Mahalanobis</i>	Anisotropic/correlated features; approximately Gaussian clusters	Requires well-conditioned covariance; sample-size sensitive; costly
<i>Geodesic</i>	Non-linear manifolds (e.g., Swiss roll) with reliable k-NN graphs	Sensitive to graph connectivity/outliers; computationally heavy
<i>Density-Norm.</i>	Heterogeneous densities; crowding mitigation; outlier robustness	Choice of k/scale matters; can overemphasize small clusters

3.4 Visualization and Analysis

While persistence diagrams and barcodes (Fig. 2) are standard tools for visual analysis when using persistent homology, we found that they did not sufficiently serve our needs for neural networks. Due to this, we identified a series of tasks and developed a set of visualization techniques that target our purpose.

3.4.1 Task Identification

We ground our task identification in the low-level analytic task taxonomy established by Amar et al. [1], which identified ten primitive operations through empirical analysis of nearly 200 data analysis questions: *Retrieve Value*, *Filter*, *Compute Derived Value*, *Find Extremum*, *Sort*, *Determine Range*, *Characterize Distribution*, *Find Anomalies*, *Cluster*, and *Correlate*. These primitives form a foundational vocabulary for describing analytic activities in information visualization systems.

Building upon this foundation, we compose four higher-level tasks specifically designed for topological analysis of neural network activations. Each task represents a composition of multiple Amar et al. primitives, applied in the context of persistent homology filtration to address the unique analytical needs of neural network interpretability. Unlike traditional static data analysis, our tasks operate on *dynamic topological features* that evolve across filtration scales, requiring coordinated application of multiple primitive operations to track hierarchical structure, assess representation quality, and identify anomalous patterns in learned representations.

[T1] Hierarchy: Understand the evolution of class clusters in activation space during the filtration process by tracking how H_0 components form, persist, merge, and disappear across scales. This task composes *Cluster* (identify connected components at each filtration level), *Characterize Distribution* (of component birth/death times), *Sort* (by persistence values), and *Determine Range* (of filtration thresholds where meaningful structure emerges). The hierarchical dendrogram reveals multi-resolution organization of learned representations.

[T2] Separability: Assess how discriminatively the network has organized different classes in activation space by measuring the degree of separation between class-specific clusters. This task composes *Cluster* (identify class groupings), *Determine*

Range (measure inter-cluster distances), *Characterize Distribution* (of within- vs. between-class distances), and *Compute Derived Value* (separation metrics at optimal filtration scales). Well-separated clusters indicate effective feature learning.

[T3] Homogeneity: Determine whether topologically coherent clusters correspond to semantically meaningful (single-class) groupings, or whether they incorrectly merge multiple classes. This task composes *Cluster* (identify persistent components), *Retrieve Value* (obtain ground-truth class labels for points within each cluster), *Compute Derived Value* (cluster purity/homogeneity metrics), and *Characterize Distribution* (of class composition within clusters). Non-homogeneous clusters suggest the network has learned representations that conflate distinct concepts.

[T4] Outliers: Identify data points with anomalous topological behavior—those that remain isolated or merge very late in the filtration—which may indicate poorly learned representations for specific inputs. This task composes *Find Anomalies* (identify outlying points), *Filter* (select late-merging or low-persistence components), *Retrieve Value* (obtain persistence/death times), and *Characterize Distribution* (of merge times to establish what constitutes “late”). Prevalent outliers suggest suboptimal model training or dataset issues.

3.4.2 Visualization Design

Based upon the analysis tools available (persistent homology), we have developed three visualization strategies, customized from common visualization types, to address the analysis tasks we have identified.

Heatmap Dendograms For the heatmap, we first get our pairwise distance matrix, and then we reorder the matrix based using Reverse-Cuthill McKee ordering. Then we build a hierarchical clustering linkage matrix from the persistence death thresholds, which is then reordered based on the RCM data point order to maintain the same data ordering. A dendrogram is a tree-like structure that shows the hierarchical clustering of the data ([T1]). In Fig. 5a, we visualize the dendrogram alongside the RCM heatmap (heatmap of the pairwise distance of datapoints with Reverse-Cuthill McKee ordering). These dendograms reveal the hierarchical clustering structure at different filtration scales, and enable us to identify critical thresholds where the clusters are formed. It also highlights how individual data points merge into larger class clusters as the distance threshold increases during the filtration process. Each major cluster is identified with a color. This enables us to identify critical thresholds where clusters emerge or disappear, and to trace how individual data points merge into larger clusters as the filtration parameter increases. The dendrogram structure captures the evolution of connectivity patterns in the data, where cluster formation and merging correspond to the underlying topological structure of the neural activations. If there exists any separability or cluster formation in the data, it can be seen in the dendrogram and the heatmap ([T2]).

Sankey-based visualizations Sankey diagrams are visualizations that help us understand the flow of data across multiple time states or filtration scales of persistent homology. We use Sankey diagrams (Fig. 5b top), as well as a compact variant (Fig. 5b bottom), to visualize the evolution of the topological features. In the visualization, we create a five-stage Sankey diagram. The initial stage contains the true labels or the ground truth. The second stage displays the clusters formed at the first threshold in the filtration process. The third and fourth stages display the most optimal thresholds across the filtration process. We define the optimal threshold as the stage that overlaps the most with the ground truth. In the fifth stage, we see that the whole point cloud forms a huge

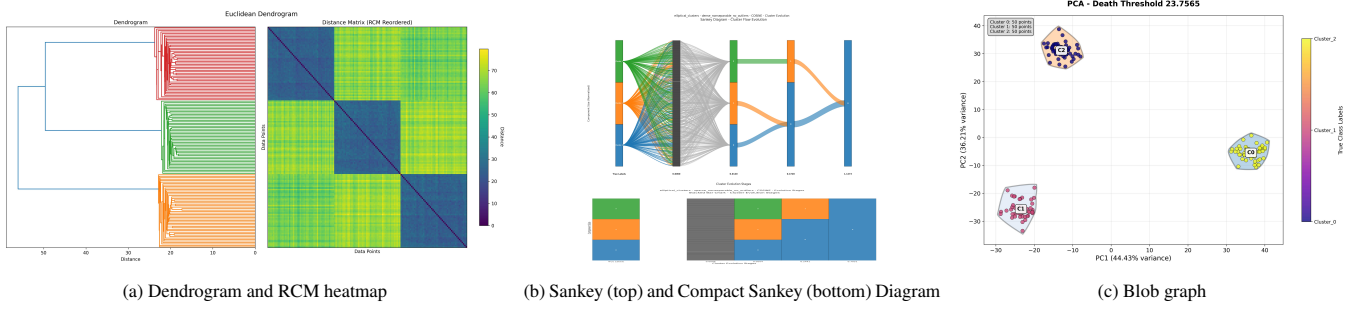


Figure 5: Examples of the visualizations used to support tasks [T1]-[T4] using persistent homology.

cluster. The Bezier curves are used to connect the clusters at the different thresholds in the Sankey diagram. These diagrams track how clusters merge and persist across different filtration stages, providing a hierarchical view of the feature evolution ([T1]), and enabling identification of cluster formations that correspond to meaningful learned representations ([T2]).

Blob Graphs Blob graphs (Fig. 5c) are scatterplots that visualize the spatial organization of activation clusters at specific death thresholds. The data layout uses linear dimensionality reduction (PCA) to project high-dimensional activations to 2D space (though any suitable dimension reduction could be used instead), with individual data points positioned according to their principal component coordinates. Data points are grouped by their ground truth class labels and colored accordingly using a distinct color palette for each class. Cluster boundaries are computed as alpha shapes or convex hulls around topological clusters (i.e., H_0 components) identified by persistent homology at the selected death threshold, with each blob colored by its cluster index. This dual encoding—individual points colored by ground truth labels and cluster boundaries derived from the PH-driven clustering—enables immediate visual assessment of cluster–class alignment quality.

Blob graphs provide multiple analytical capabilities. By observing the homogeneity of labels within each blob (persistent component at ϵ^*), we can qualitatively assess how well the PH-derived clusters align with the semantic class structure of the data, spatially forming cohesive groups in the learned representation space ([T2] and [T3]). Further, points that fall outside any blob or belong to a component dominated by another class can be viewed as outliers or potential misclassifications—often corresponding to late-merging or low-persistence structures—indicating limitations in the network’s feature learning ([T4]). Finally, though not a primary task, the visualization supports comparative analysis across layers, distance metrics, robustness, and compression techniques, allowing us to relate representational quality to the stability and mergers of H_0 features across the filtration.

3.5 Interpretability Workflow

The user can load a PyTorch model and a dataset, and then select the relevant activation layers to visualize in the HOLE library. The forward hooks are placed at the selected layers, and the activations are extracted after a forward pass through the model. The activations are extracted and sent through a filtration function, and persistent homology is computed. The filtration is performed based on the user’s choice of distance metric. Each distance is unique and reveals a different geometric and semantic aspect of the learned representations. The resulting topological features, particularly the birth and death of connected components across filtration scales, are tracked to understand how the network organizes and separates different classes of data. The filtration data is returned, and the user can visualize the data using the following methods:

1. Sankey-based flow diagrams, which are useful to track cluster evolution.
2. Blob graphs, which reveal the spatial organization of clusters at a certain threshold.
3. Dendrogram heatmaps, which give an overview of the filtration process.

Clusters with a low datapoint count are considered noise or outliers. Disconnected components that persist for a long time as a separate cluster are considered to be outliers. Such clusters are filtered out. Clusters that persist for a long time are considered to be centroids of the class. In earlier layers, clusters are likely to be noisy, and in later layers, clusters are likely to be the learned representations of the class. This can be seen using the different Sankey-based visualizations. By treating these connected components as clusters, we can evaluate their alignment with semantic class labels. This allows us to examine whether the neural network’s representation space induces a natural partitioning of the data, and at what filtration scales these partitions become meaningful.

4 EVALUATIONS

4.1 Implementation

We have implemented HOLE in Python. The hook functions are implemented using PyTorch’s module-level forward hooks, which allow capturing outputs during a forward pass without altering the network architecture. The input data is fed into the neural network, and the activations are recorded at each layer. For a given batch of inputs and a specified network layer, we collect the layer activations and flatten them to form vectors in \mathbb{R}^d , where d is the number of output units in that layer. The resulting $N \times d$ matrix defines a point cloud of N points in d -dimensional space. These probed intermediate activations then act as point clouds for the persistent homology pipeline, which is then used to study the layer topology. We then use GUDHI [50] to compute the persistent homology. Source code is included with our submission for review only, and it will be released as an open-source repository upon publication.

4.2 Dataset and Network Architectures

The primary dataset used in our experiments is CIFAR-10 [39], a widely adopted benchmark in computer vision for image classification. It consists of 60,000 images at a resolution of 32×32, evenly distributed across 10 mutually exclusive classes: airplane, automobile, bird, cat, deer, dog, frog, horse, ship, and truck. The standard split allocates 50,000 images for training and 10,000 for testing.

We evaluated HOLE for interpretability across multiple neural network architectures to demonstrate its model-agnostic capabilities. *ResNet Family:* We primarily focus on ResNet-18 as our baseline architecture, with additional experiments on ResNet-34, and ResNet-50 [30] to analyze how network depth affects topological

features and interpretability patterns. *Vision Transformer (ViT)*: We ran our experiments on ViT-B/16 and ViT-L/16 models [16], which allowed us to explore transformer architectures.

4.3 Application 1: Learned Representation Analysis

Exploring the model’s learned representations is a key aspect of understanding its behavior. Performing comparative analysis across layers helps understand what layers induce disentanglement of class representations. For example, using different distance metrics yields different insights (Fig. 6). The decision boundaries and class separability are much more prominent in later layers of networks in comparison to earlier layers. We can see that by comparing layers 10 and 11 (Figs. 6b and 6d, respectively). In this case, the class separability is much more prominent in layer 11 (Fig. 6d). Similarly, the clustering is more pronounced in later layers than in the earliest layers (Figs. 6e and 6f). Additional results are shown in the Appendix.

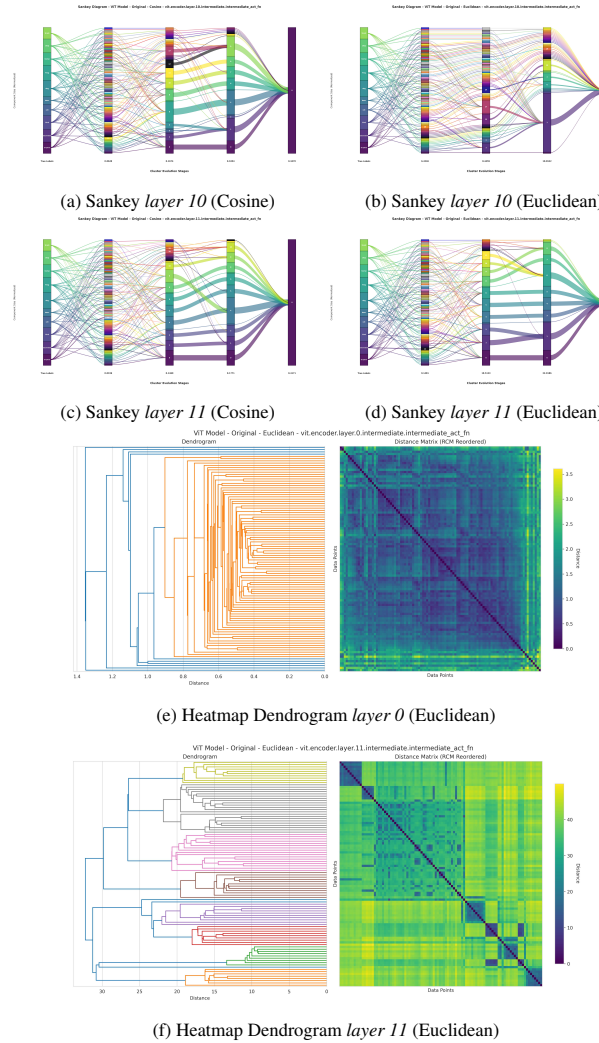


Figure 6: Comparison of (a-d) Sankey diagrams for ViT encoder layers 10 and 11 using different distance metrics and (e-f) heatmap dendograms between layers 0 and 11.

4.4 Application 2: Robustness Analysis Under Noise

Using HOLE, one can perform also robustness assessment along with interpretability through topological analysis of model behavior

under various perturbations.

We performed comprehensive robustness assessment through automated topological analysis of model behavior under various perturbations. Using HOLE, we systematically evaluate how different noise types affect the learned representations’ topological structure across multiple noise categories (Fig. 7). We pass corrupted inputs and generate comparative visualizations that reveal which topological features remain stable and which are vulnerable to specific corruption patterns. Technical specifications for each noise model are provided in the Appendix.

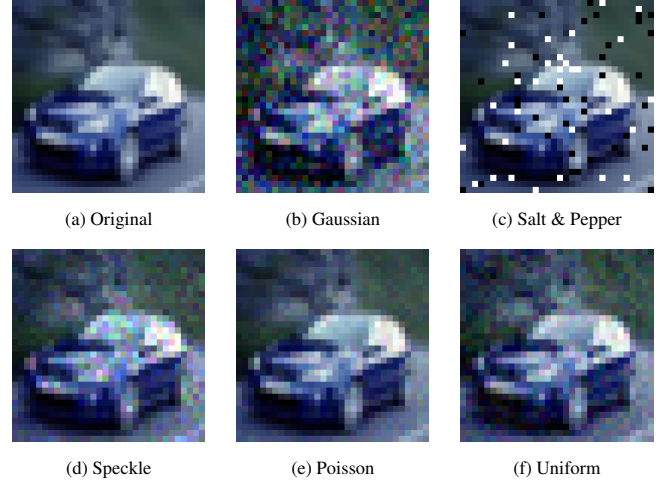


Figure 7: Input noise robustness evaluation on CIFAR-10. Various noise types are applied to assess model robustness and topological stability under different perturbation scenarios.

Speckle Noise Impact Analysis Our analysis reveals that speckle noise significantly degrades topological structure in deep layer representations. Comparing the blob visualizations, we observe that the uniform clustering structure present in clean data (Fig. 8a) becomes fragmented under speckle corruption (Fig. 8c). The class separability deteriorates markedly, with cluster boundaries becoming less distinct and more overlapping. This degradation is consistently observed across visualization methods. The Sankey diagrams (Figs. 8b and 8d) demonstrate reduced flow coherence between filtration stages, indicating that topological features become less stable under speckle noise. Quantitatively, the clustering purity drops from 0.87 in clean data to 0.62 under speckle noise, while the number of persistent components increases by 34%, suggesting noise-induced fragmentation of the representation space.

Comparative Robustness Analysis Our systematic evaluation across noise types reveals distinct vulnerability patterns in the learned representations. Gaussian and uniform noise show moderate impact on topological structure, with clustering purity decreasing by approximately 15-20%. Salt-and-pepper noise demonstrates the most severe disruption, fragmenting cluster boundaries and reducing purity by up to 45%. Poisson noise exhibits intermediate effects, with degradation proportional to the noise-to-signal ratio.

Implications for Model Robustness These findings indicate that multiplicative noise types (speckle) and impulse noise (salt-and-pepper) pose greater threats to the topological integrity of learned representations than additive noise types. The consistent degradation patterns observed across multiple visualization methods suggest that topological analysis provides a reliable framework for assessing model robustness beyond traditional accuracy metrics. This analysis demonstrates how HOLE enables researchers to iden-

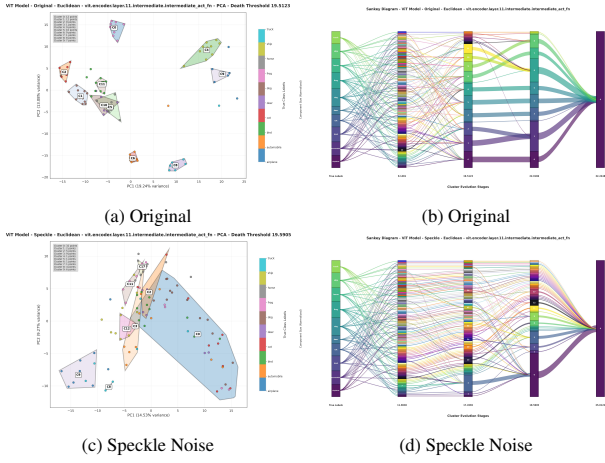


Figure 8: Comparison of (left) Blob graphs and (right) Sankey diagrams with (top) original and (bottom) speckle-noised images.

toify specific vulnerabilities in deep learning models and guide the development of more robust architectures.

4.5 Application 3: Model Compression Techniques

Model compression techniques such as pruning and quantization are essential for deploying neural networks in resource-constrained environments. However, these techniques fundamentally alter network parameters and may affect the quality of learned representations. HOLE provides the necessary visualization techniques to understand the impact of compression techniques on the topological structure to interpret the neural activations.

Understanding these topological changes is crucial because the clustering patterns and connectivity structures in activation spaces directly reflect how well the network has learned to organize and separate different concepts. When compression disrupts these patterns, it may indicate a loss of representational quality that standard accuracy metrics might not capture.

4.5.1 Pruning

Pruning is a model compression technique that helps sparsify a network by systematically removing redundant or less important parameters by setting them to zero [42, 29]. The fundamental principle behind pruning is based on the observation that many neural networks are over-parameterized [22], containing numerous weights that contribute minimally to the final output. By identifying and removing these parameters, we can achieve significant reductions in model size and computational requirements while maintaining comparable performance.

Pruning typically involves three main steps. First, during *Importance Scoring*, each parameter is assigned a score reflecting its contribution to the network’s performance. Next, during *Selection*, parameters with scores below a certain threshold are marked for removal. Finally, during *Removal*, the selected parameters are set to zero or completely eliminated from the network structure [8].

There are several variants of pruning strategies. With magnitude-based pruning, parameters are ranked by their absolute values, with smaller weights considered less important and removed first [28]. Structured pruning removes entire channels, filters, or layers [43, 45], while unstructured pruning removes individual weights regardless of their position in the network architecture [48]. Finally, global pruning considers all parameters across the entire network when making removal decisions [28], while layer-wise pruning makes decisions independently within each layer [53].

Pruning Experiments We apply magnitude-based unstructured pruning [28] to remove weights below a threshold τ , effectively setting $w_{ij} = 0$ for $|w_{ij}| < \tau$. This sparsification process reduces the effective dimensionality of activation spaces and may eliminate critical topological connections. We evaluate pruning ratios from 10% to 90% and analyze how the resulting sparse networks maintain or lose persistent homological features across layers. We implement two distinct pruning strategies to analyze their differential impact on topological structure:

- **30% Global Unstructured Pruning:** Applies L1 magnitude-based weight removal across the entire network, creating a sparse model with 30% of weights set to zero based on global magnitude ranking. This approach ensures that the most important weights across the entire network are preserved, regardless of their layer location.
- **20% Layer-wise Unstructured Pruning:** Prunes weights independently within each layer using L1 magnitude criteria, removing 20% of weights per layer while maintaining local structural balance. This strategy preserves the relative importance distribution within each layer but may remove globally important weights.

Our topological analysis reveals how each pruning strategy affects the formation and stability of activation clusters. In Fig. 9, ResNet-34 exhibits clear, multi-cluster structure before pruning that collapses into a single dominant cluster after pruning (loss of intermediate merges, many components merging early). This indicates that pruning destroyed discriminative substructure in the activation manifold rather than merely sparsifying parameters. The comparison between global and layer-wise pruning strategies is particularly informative for understanding how sparsity distribution impacts learned representations and whether certain topological features are more resilient to different pruning approaches. Having models which are more robust to pruning is important for deployment in real-world applications. Before pruning there was stable cluster formation; after pruning, the activation space degenerates into a single dominant cluster—topologically visible as early H_0 coalescence and shallow dendrogram structure.

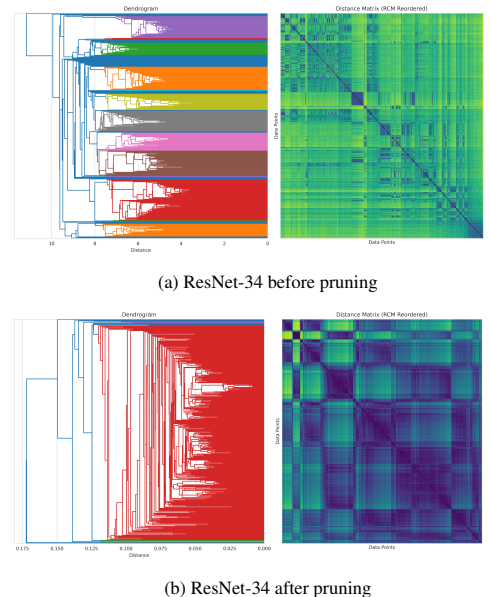


Figure 9: ResNet-34 persistent dendrogram + heatmap before and after pruning (new plots).

4.5.2 Quantization

Quantization is a compression technique that reduces the precision of numerical representations used in neural networks, typically converting floating-point weights and activations to lower bit-width representations [23]. This process significantly reduces memory requirements and computational complexity, making models more suitable for deployment on resource-constrained devices such as mobile phones and embedded systems [33].

The quantization process involves mapping continuous floating-point values to a discrete set of quantized values [38]. The most common approach is uniform quantization, where the range of possible values is divided into equally-spaced intervals. For a given floating-point value x , the quantized representation q is computed as: $q = \text{round}(\frac{x-z}{s})$, where s is the scale factor that determines the spacing between quantized levels, and z is the zero-point that ensures the quantization scheme can represent zero exactly [33].

Several quantization strategies exist. Post-training quantization is applied after the model has been fully trained, requiring no re-training but potentially leading to accuracy degradation [4, 56]. Quantization-aware training incorporates quantization effects during the training process, typically achieving better accuracy preservation [33, 20]. Dynamic quantization determines scale and zero-point parameters at runtime [74], while static quantization precomputes these parameters using calibration data [52]. Weight-only quantization applies only to model parameters [14], while full quantization includes both weights and activations [33].

The discrete nature of quantized representations introduces step-wise perturbations that may fundamentally alter the continuous structure of activation manifolds, making it particularly important to understand their topological implications [75].

Quantization Experiments We implement post-training quantization [28, 38], mapping full-precision weights and activations to lower bit-widths using uniform quantization. We examine 8-bit, 4-bit, and 2-bit quantization schemes and their impact on the stability of topological features. Specifically, we evaluate INT8 Dynamic Quantization. It reduces the precision of linear layer weights to 8-bit integers during inference while keeping activations in full precision. This represents a practical deployment scenario that balances compression efficiency with accuracy preservation. Our analysis focuses on how quantization-induced discretization affects the continuity of activation spaces and the stability of persistent homological features. We particularly investigate whether the step-wise nature of quantized representations creates artificial clustering patterns or disrupts meaningful topological structures learned during training; in practice, quantization tends to snap nearby points (altering local neighborhoods), suppress low-variance directions, and sever thin connectors, which shifts several H_0 birth-death orderings. In Fig. 10, the “after” view shows widespread cluster breakup, spurious overlaps, and the disappearance of bridging structure rather than benign tightening.

These compression levels represent practical deployment scenarios where significant model reduction is needed while maintaining reasonable performance. Our topological analysis reveals how each technique affects the formation and stability of activation clusters, providing insights into which compression approaches preserve meaningful representational structure and which may disrupt important feature relationships.

In our runs, INT8 was not acceptable: the before/after blobs reveal fragmentation and mixed-class blobs; Sankey flows (not shown) lose stage-to-stage coherence with diffuse, noisy links; and persistence dendrograms proliferate shallow branches with delayed merges. Together these views show that INT8 degraded the representational topology; mitigation likely requires calibration or quantization-aware training.

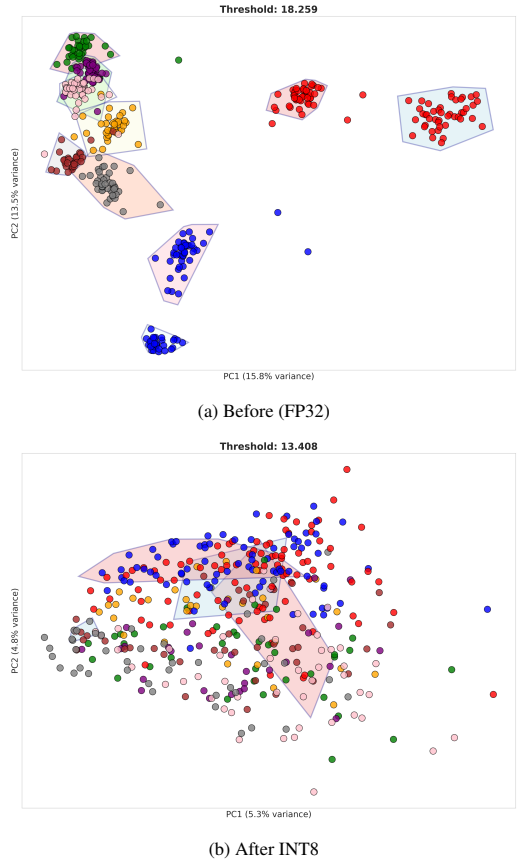


Figure 10: Blob visualizations of ViT encoder layer 11 activations before and after INT8 dynamic quantization.

5 DISCUSSION

This work presents HOLE (Homological Observation of Latent Embeddings), a library that leverages persistent homology to provide interpretable analysis of deep neural network representations. Our approach addresses a fundamental challenge in modern machine learning: understanding the internal mechanisms of complex models that have achieved remarkable performance but remain as black boxes. By treating neural network activations as point clouds and applying topological data analysis through Vietoris-Rips filtrations, we demonstrate that persistent homology can reveal meaningful structural patterns in learned representations that are invisible to traditional interpretability methods. The HOLE’s model-agnostic nature allows it to be applied across diverse architectures—from convolutional networks like ResNet to transformer-based models like ViT, while providing consistent insights into representation quality, layer-wise feature evolution, and model robustness. Our experimental validation on CIFAR-10 across multiple network architectures shows that topological features can effectively capture class separation dynamics, identify critical layers where semantic clustering emerges, and reveal how different distance metrics (Euclidean, cosine, Mahalanobis, and relative neighborhood normalization) expose different aspects of the representational structure. The visualization strategies we employ, including multiple variants of the Sankey diagrams for tracking cluster evolution across layers and force-directed graphs for spatial representation of topological features, provide intuitive interfaces for practitioners to understand complex high-dimensional phenomena.

The implications of this work extend beyond interpretability to practical applications in model development and deployment. Our

robustness analysis demonstrates that topological signatures can serve as early indicators of model vulnerability to various noise types and perturbations, offering a complementary perspective to traditional accuracy-based evaluation metrics. The framework’s ability to analyze model compression techniques—including pruning and quantization—through the lens of topological preservation provides a principled approach to efficient model design that maintains representational integrity. Furthermore, our findings suggest that persistent homology can guide architectural decisions by identifying layers that contribute most significantly to semantic organization, potentially informing network design and optimization strategies. The stability properties of persistent homology, combined with its robustness to noise and minor perturbations, make it particularly suitable for analyzing real-world deployed models where data distribution shifts and adversarial perturbations are common concerns. As deep learning models continue to be deployed in critical applications requiring transparency and reliability, topological analysis offers a mathematically grounded framework for understanding and validating model behavior. The comprehensive research agenda we outline for future work—including manifold-aware distance metrics, temporal extensions for sequential models, and domain-specific applications in scientific computing—positions persistent homology as a fundamental tool in the interpretable machine learning toolkit, bridging the gap between theoretical understanding and practical model analysis.

6 FUTURE WORK

The HOLE library presented here can be extended in several ways for future work.

Methodological Advances Current distance formulations assume Euclidean geometry in activation space. We propose investigating geodesic distances on learned manifolds and developing density-adaptive metrics that account for local neighborhood structure in high-dimensional embeddings [47]. Systematic investigation of topological changes under adversarial perturbations [69] may reveal fundamental principles of adversarial vulnerability and inform the development of topology-based defense mechanisms.

Additional Network Architectures Recurrent and transformer architectures process sequential information through complex temporal dependencies. We propose developing formulations that can capture the evolution of topological features across sequence positions, providing insights into memory formation and temporal representation learning. Extending our framework to generative architectures presents unique opportunities. Analysis of latent space topology in variational autoencoders [37] and the generator manifold in generative adversarial networks [26] could provide insights into mode collapse, sample diversity, and generation quality.

Scalability and Computational Efficiency Adapting methods from spatial data analysis [65], we propose incorporating kernel density estimation for persistence diagram visualization. This approach would identify regions of high topological activity and provide intuitive representations of feature density distributions. Computational complexity represents a significant barrier to applying topological analysis to large networks and datasets. We will consider investigating coresnet approximations [21] that maintain topological fidelity while reducing computational requirements, enabling analysis of production-scale models.

ACKNOWLEDGMENTS

The authors wish to thank A, B, and C. This work was supported in part by a grant from XYZ.

REFERENCES

- [1] R. Amar, J. Eagan, and J. Stasko. Low-level components of analytic activity in information visualization. In *IEEE Symposium on Information Visualization*, pp. 111–117, 2005. doi: 10.1109/INFVIS.2005.1532136 2, 5
- [2] S. Bach, A. Binder, G. Montavon, F. Klauschen, K.-R. Müller, and W. Samek. On pixel-wise explanations for non-linear classifier decisions by layer-wise relevance propagation. *PloS one*, 10(7), 2015. doi: 10.1371/journal.pone.0130140 2
- [3] R. Ballester, X. Arnal, C. Casacuberta, M. Madadi, C. Corneau, and S. Escalera. Predicting the generalization gap in neural networks using topological data analysis. *Neurocomputing*, 2024. doi: 10.1016/j.neucom.2024.127787 3
- [4] R. Banner, Y. Nahshan, E. Hoffer, and D. Soudry. Post training 4-bit quantization of convolutional networks for rapid-deployment. In *Advances in Neural Information Processing Systems*, vol. 32, 2019. 9
- [5] S. Barocas and A. D. Selbst. *Big data’s disparate impact*, vol. 104. HeinOnline, 2016. doi: 10.2139/ssrn.2477899 1
- [6] D. Bau, B. Zhou, A. Khosla, A. Oliva, and A. Torralba. Network dissection: Quantifying interpretability of deep visual representations. In *IEEE Conference on Computer Vision and Pattern Recognition*, pp. 6541–6549, 2017. doi: 10.1109/CVPR.2017.354 2
- [7] T. Birdal, A. Lou, L. Guibas, and U. Simsekli. Intrinsic dimension, persistent homology and generalization in neural networks. In *Advances in Neural Information Processing Systems*, 2021. 3
- [8] D. Blalock, J. J. G. Ortiz, J. Frankle, and J. Guttag. What is the state of neural network pruning? *Machine Learning and Systems*, 2:129–146, 2020. 8
- [9] P. Bubenik. Statistical topological data analysis using persistence landscapes. *Journal of Machine Learning Research*, 16:77–102, 2015. 2
- [10] G. Carlsson. Topology and data. *Bulletin of the American Mathematical Society*, 46(2):255–308, 2009. doi: 10.1090/S0273-0979-09-01249-X 4
- [11] M. Carrière, M. Cuturi, and S. Oudot. Sliced wasserstein kernel for persistence diagrams. In *International Conference on Machine Learning*, pp. 664–673, 2017. 2
- [12] M. Carrière, M. Cuturi, S. Oudot, and B. Rieck. Perslay: A neural network layer for persistence diagrams and new graph topological signatures. In *AISTATS*, 2020. 3
- [13] D. Cohen-Steiner, H. Edelsbrunner, and J. Harer. Stability of persistence diagrams. *Discrete & Computational Geometry*, 37(1):103–120, 2007. doi: 10.1007/s00454-006-1276-5 2
- [14] T. Dettmers, M. Lewis, Y. Belkada, and L. Zettlemoyer. Gpt3.int8(): 8-bit matrix multiplication for transformers at scale. *Advances in Neural Information Processing Systems*, 35:30318–30332, 2022. 9
- [15] J. Devlin, M.-W. Chang, K. Lee, and K. Toutanova. Bert: Pre-training of deep bidirectional transformers for language understanding. *arXiv preprint*, 2018. 1
- [16] A. Dosovitskiy, L. Beyer, A. Kolesnikov, D. Weissenborn, X. Zhai, T. Unterthiner, M. Dehghani, M. Minderer, G. Heigold, S. Gelly, J. Uszkoreit, and N. Houlsby. An image is worth 16x16 words: Transformers for image recognition at scale. In *International Conference on Learning Representations*, 2021. 7
- [17] H. Edelsbrunner and J. Harer. *Computational topology: an introduction*. American Mathematical Soc., 2010. 4
- [18] H. Edelsbrunner, D. Letscher, and A. Zomorodian. Topological persistence and simplification. *Discrete & Computational Geometry*, 28(4):511–533, 2002. doi: 10.1109/SFCS.2000.892133 2, 4
- [19] D. Erhan, Y. Bengio, A. Courville, and P. Vincent. Visualizing higher-layer features of a deep network. In *International Conference on Machine Learning*, pp. 341–348, 2009. 2
- [20] S. K. Esser, J. L. McKinstry, D. Bablani, R. Appuswamy, and D. S. Modha. Learned step size quantization. In *International Conference on Learning Representations*, 2020. 9
- [21] D. Feldman, M. Schmidt, and C. Sohler. Turning big data into tiny data: Constant-size coresets for k-means, pca, and projective clustering. *SIAM Journal on Computing*, 49(3):601–657, 2020. doi: 10.1137/18M1209854 10

[22] J. Frankle and M. Carbin. The lottery ticket hypothesis: Finding sparse, trainable neural networks. In *International Conference on Learning Representations*, 2019. 8

[23] A. Gholami, S. Kim, Z. Dong, Z. Yao, M. W. Mahoney, and K. Keutzer. A survey of quantization methods for efficient neural network inference. *arXiv preprint*, 2021. doi: 10.1201/9781003162810-13 9

[24] R. Ghrist. Barcodes: The persistent topology of data. *Bulletin of the American Mathematical Society*, 45(1):61–75, 2008. doi: 10.1090/S0273-0979-07-01191-3 2

[25] I. Goodfellow, Y. Bengio, and A. Courville. *Deep learning*. MIT press, 2016. 1

[26] I. Goodfellow, J. Pouget-Abadie, M. Mirza, B. Xu, D. Warde-Farley, S. Ozair, A. Courville, and Y. Bengio. Generative adversarial nets. In *Advances in Neural Information Processing Systems*, vol. 27, 2014. 10

[27] A. Gutiérrez-Fandiño, D. Pérez-Fernández, J. Armengol-Estabé, and M. Villegas. Persistent homology captures the generalization of neural networks without a validation set. *arXiv preprint*, 2021. 3

[28] S. Han, H. Mao, and W. J. Dally. Deep compression: Compressing deep neural networks with pruning, trained quantization and huffman coding. In *International Conference on Learning Representations*, 2016. ICLR 2016 (oral). 8, 9

[29] B. Hassibi and D. G. Stork. Second order derivatives for network pruning: Optimal brain surgeon. *Advances in Neural Information Processing Systems*, 5, 1993. 8

[30] K. He, X. Zhang, S. Ren, and J. Sun. Deep residual learning for image recognition. In *IEEE Conference on Computer Vision and Pattern Recognition*, pp. 770–778, 2016. doi: 10.1109/CVPR.2016.90 6

[31] C. Hofer, R. Kwitt, M. Niethammer, and A. Uhl. Deep learning with topological signatures. In *Advances in Neural Information Processing Systems*, 2017. 3

[32] F. Hohman, H. Park, C. Robinson, and D. H. Chau. Summit: Scaling deep learning interpretability by visualizing activation and attribution summarizations. *IEEE Transactions on Visualization and Computer Graphics*, 26(1):1–12, 2020. doi: 10.1109/TVCG.2019.2934659 3

[33] B. Jacob, S. Kligys, B. Chen, M. Zhu, M. Tang, A. Howard, H. Adam, and D. Kalenichenko. Quantization and training of neural networks for efficient integer-arithmetic-only inference. In *IEEE Conference on Computer Vision and Pattern Recognition*, pp. 2704–2713, 2018. doi: 10.1109/CVPR.2018.00286 9

[34] M. Kahng, P. Y. Andrews, A. Kalro, and D. H. Chau. Activis: Visual exploration of industry-scale deep neural network models. *IEEE Transactions on Visualization and Computer Graphics*, 24(1):88–97, 2018. doi: 10.1109/TVCG.2017.2744718 3

[35] A. E. Khandani, A. J. Kim, and A. W. Lo. Consumer credit-risk models via machine-learning algorithms. *Journal of Banking & Finance*, 34(11):2767–2787, 2010. 1

[36] B. Kim, M. Wattberg, J. Gilmer, C. Cai, J. Wexler, F. Viegas, and R. Sayres. Interpretability beyond feature attribution: Quantitative testing with concept activation vectors (tcav). In *International Conference on Machine Learning*, pp. 2668–2677, 2018. 2

[37] D. P. Kingma and M. Welling. Auto-encoding variational bayes. *arXiv preprint*, 2013. 10

[38] R. Krishnamoorthi. Quantizing deep convolutional networks for efficient inference: A whitepaper. *arXiv preprint*, 2018. 9

[39] A. Krizhevsky. Learning multiple layers of features from tiny images. Technical report, University of Toronto, 2009. Technical Report. 6

[40] A. Krizhevsky, I. Sutskever, and G. E. Hinton. Imagenet classification with deep convolutional neural networks. In *Advances in Neural Information Processing Systems*, pp. 1097–1105, 2012. doi: 10.1145/3065386 1

[41] Y. LeCun, Y. Bengio, and G. Hinton. Deep learning. *Nature*, 521(7553):436–444, 2015. doi: 10.1038/nature14539 1

[42] Y. LeCun, J. Denker, and S. Solla. Optimal brain damage. *Advances in Neural Information Processing Systems*, 2, 1989. 8

[43] H. Li, A. Kadav, I. Durdanovic, H. Samet, and H. P. Graf. Pruning filters for efficient convnets. In *International Conference on Learning Representations*, 2017. 8

[44] M. Liu, J. Shi, Z. Li, C. Li, J. Zhu, and S. Liu. Towards better analysis of deep convolutional neural networks. *IEEE Transactions on Visualization and Computer Graphics*, 23(1):831–840, 2017. doi: 10.1109/TVCG.2016.2598831 3

[45] Z. Liu, J. Li, Z. Shen, G. Huang, S. Yan, and C. Zhang. Learning efficient convolutional networks through network slimming. In *IEEE International Conference on Computer Vision*, pp. 2736–2744, 2017. doi: 10.1109/ICCV.2017.298 8

[46] F. J. López Iturriaga and I. P. Sanz. Machine learning: Challenges, lessons, and opportunities in credit risk modeling. *Moody's Analytics Risk Perspectives*, 2013. 1

[47] A. Lou, D. Lim, I. Katsman, L. Huang, Q. Jiang, S.-N. Lim, and C. De Sa. Neural manifold ordinary differential equations. *Advances in Neural Information Processing Systems*, 33:17548–17558, 2020. 10

[48] C. Louizos, M. Welling, and D. P. Kingma. Learning sparse neural networks through l_0 regularization. In *International Conference on Learning Representations*, 2018. 8

[49] S. M. Lundberg and S.-I. Lee. A unified approach to interpreting model predictions. In *Advances in Neural Information Processing Systems*, vol. 30, pp. 4765–4774, 2017. 2

[50] C. Maria, J.-D. Boissonnat, M. Glisse, and M. Yvinec. The gudhi library: Simplicial complexes and persistent homology. In *International Congress on Mathematical Software (ICMS)*, pp. 167–174, 2014. doi: 10.1007/978-3-662-44199-2_28 2, 6

[51] N. Mehrabi, F. Morstatter, N. Saxena, K. Lerman, and A. Galstyan. A survey on bias and fairness in machine learning. *ACM Computing Surveys (CSUR)*, 54(6):1–35, 2021. doi: 10.1145/3457607 1

[52] S. Migacz. 8-bit inference with tensorrt. In *GPU Technology Conference*, 2017. 9

[53] P. Molchanov, S. Tyree, T. Karras, T. Aila, and J. Kautz. Pruning convolutional neural networks for resource efficient inference. In *International Conference on Learning Representations*, 2017. 8

[54] C. Molnar. *Interpretable machine learning*. Lulu. com, 2020. 1

[55] M. Moor, M. Horn, B. Rieck, and K. Borgwardt. Topological autoencoders. In *International Conference on Machine Learning*, 2020. 3

[56] M. Nagel, M. v. Baalen, T. Blankevoort, and M. Welling. Data-free quantization through weight equalization and bias correction. In *IEEE International Conference on Computer Vision*, pp. 1325–1334, 2019. doi: 10.1109/ICCV.2019.00141 9

[57] C. Olah, A. Mordvintsev, and L. Schubert. Feature visualization. *Distill*, 2017. doi: 10.23915/distill.00007 2

[58] E. Purvine, D. Brown, B. Jefferson, C. Joslyn, B. Praggastis, A. Rathore, M. Shapiro, B. Wang, and Y. Zhou. Experimental observations of the topology of convolutional neural network activations. *AAAI Conference on Artificial Intelligence*, 37(8):9470–9479, 2023. doi: 10.1609/aaai.v37i8.26134 2

[59] E. Purvine et al. Experimental observations of the topology of convolutional neural network activations. In *IEEE Symposium on Visualization for Cyber Security*, 2022. doi: 10.1609/aaai.v37i8.26134 3

[60] A. Rajkomar, E. Oren, K. Chen, A. M. Dai, N. Hajaj, M. Hardt, P. J. Liu, X. Liu, J. Marcus, M. Sun, et al. Scalable and accurate deep learning with electronic health records. *NPJ Digital Medicine*, 1(1):1–10, 2018. doi: 10.1038/s41746-018-0029-1 1

[61] M. T. Ribeiro, S. Singh, and C. Guestrin. “why should i trust you?” explaining the predictions of any classifier. In *ACM SIGKDD International Conference on Knowledge Discovery and Data Mining*, pp. 1135–1144, 2016. doi: 10.18653/v1/N16-3020 2

[62] B. Rieck, M. Togninalli, M. Bianchini, J. M. Buhmann, C. Kenel, D. Lun, A. Radeghieri, C. Ertle, and D. H’ottger. Neural persistence: A complexity measure for deep neural networks using algebraic topology. In *International Conference on Learning Representations*, 2019. ICLR. 3

[63] C. Rudin. Stop explaining black box machine learning models for high stakes decisions and use interpretable models instead. *Nature Machine Intelligence*, 1(5):206–215, 2019. doi: 10.1038/s42256-019-0048-x 1

[64] R. R. Selvaraju, M. Cogswell, A. Das, R. Vedantam, D. Parikh, and D. Batra. Grad-cam: Visual explanations from deep networks via gradient-based localization. In *IEEE International Conference on Computer Vision*, pp. 618–626, 2017. doi: 10.1007/s11263-019-01228-7 2

[65] B. W. Silverman. *Density Estimation for Statistics and Data Analysis*. Routledge, 1st ed., 2018. doi: 10.1201/9781315140919 [10](#)

[66] G. Singh, F. Mémoli, G. E. Carlsson, et al. Topological methods for the analysis of high dimensional data sets and 3d object recognition. *PBG@ Eurographics*, 2:091–100, 2007. [2](#)

[67] D. Smilkov, N. Thorat, B. Kim, F. Viégas, and M. Wattenberg. Smoothgrad: removing noise by adding noise. *arXiv preprint*, 2017. [2](#)

[68] M. Sundararajan, A. Taly, and Q. Yan. Axiomatic attribution for deep networks. *International Conference on Machine Learning*, pp. 3319–3328, 2017. [2](#)

[69] C. Szegedy, W. Zaremba, I. Sutskever, J. Bruna, D. Erhan, I. Goodfellow, and R. Fergus. Intriguing properties of neural networks. *arXiv preprint*, 2013. [10](#)

[70] E. J. Topol. High-performance medicine: the convergence of human and artificial intelligence. *Nature medicine*, 25(1):44–56, 2019. doi: 10.1038/s41591-018-0300-7 [1](#)

[71] Z. J. Wang, R. Turko, O. Shaikh, H. Park, N. Das, F. Hohman, M. Kahng, and D. H. Chau. Cnn explainer: Learning convolutional neural networks with interactive visualization. *IEEE Transactions on Visualization and Computer Graphics*, 27(1):1396–1406, 2021. doi: 10.1109/TVCG.2020.3030418 [3](#)

[72] S. Watanabe and H. Yamana. Topological measurement of deep neural networks using persistent homology. *Complexity*, 2021. doi: 10.1007/s10472-021-09761-3 [3](#)

[73] B. Wheeler, V. Bouza, and P. Bubenik. Activation landscapes as a topological summary of neural network performance. In *International Conference on Machine Learning*, 2021. doi: 10.1109/BigData52589.2021.9671368 [3](#)

[74] H. Wu, P. Judd, X. Zhang, M. Isaev, and P. Micikevicius. Integer quantization for deep learning inference: Principles and empirical evaluation. *arXiv preprint*, 2020. [9](#)

[75] Z. Yao, Z. Dong, Z. Zheng, A. Gholami, J. Yu, E. Tan, L. Wang, Q. Huang, Y. Wang, M. Mahoney, et al. Hawq-v3: Dyadic neural network quantization. In *International Conference on Machine Learning*, pp. 11875–11886, 2021. [9](#)

[76] M. D. Zeiler and R. Fergus. Visualizing and understanding convolutional networks. In *European Conference on Computer Vision*, pp. 818–833, 2014. doi: 10.1007/978-3-319-10590-1_53 [2](#)

[77] A. Zomorodian and G. Carlsson. Computing persistent homology. *Discrete & Computational Geometry*, 33(2):249–274, 2005. doi: 10.1145/997817.997870 [2](#)